

Chapter 3

NEWFIRM Camera

Version 1.0, May 2009

In This Chapter...

Instrument Overview	3-1
Data Products	3-10
Calibration	3-18
Sources of Error	3-28
References & Further Information	3-31

The NEWFIRM camera was placed in routine operation at KPNO in late 2007, and definitive technical and performance information is still being assembled. The material presented here is drawn primarily from the *NEWFIRM Quick Guide for Proposal Preparation* (Probst 2008), and from the *NEWFIRM Quick Reduce Pipeline and Data Analysis Tools* notes by Dickinson, et al. (2008). Interested users should consult these documents for details of the instrument description and pipeline operation. Additional resources¹ are cited throughout this chapter, and are listed along with other background material in the last section.

3.1 INSTRUMENT OVERVIEW

The NOAO Extremely Wide-Field Infrared Mosaic (NEWFIRM) camera has rapidly become one of the most heavily used instruments offered by NOAO because of its excellent infrared (IR) sensitivity and very large field of view. NEWFIRM is planned to be used at both the Mayall 4-m on Kitt Peak and the Blanco 4-m telescope on Cerro Tololo, in alternating campaigns. This chapter describes both usages of the camera.

1. See the NEWFIRM instrument Web site at <http://www.noao.edu/ets/newfirm/>

3.1.1 Instrument Capabilities & Design

The NEWFIRM camera is a near-IR imager with a wide field of view (FoV) and a large focal-plane array (FPA) containing four InSb detectors with a total of 4096×4096 pixels. A schematic of the instrument is shown in Figure 3.1. The detectors have quantum efficiency (QE) near 90% over the wavelength range 0.8–4.5 μm , with the exception of one detector (SN019), where a thicker anti-reflection coating degrades the QE by $\sim 10\%$ shortward of $\sim 2.5 \mu\text{m}$. There are two filter wheels, each with 7 slots, that can hold a subset of the available filters for NEWFIRM. The filter sets² include standard broad bandpasses, such as JHK_s , mediumband filters, and a few narrowband filters including [Fe II] 1.64 μm , H₂ 2.12 μm and Br γ 2.17 μm . Since the detector has high QE well beyond the bandpasses of the current filter set, blocking filters are sometimes used to minimize red leak.

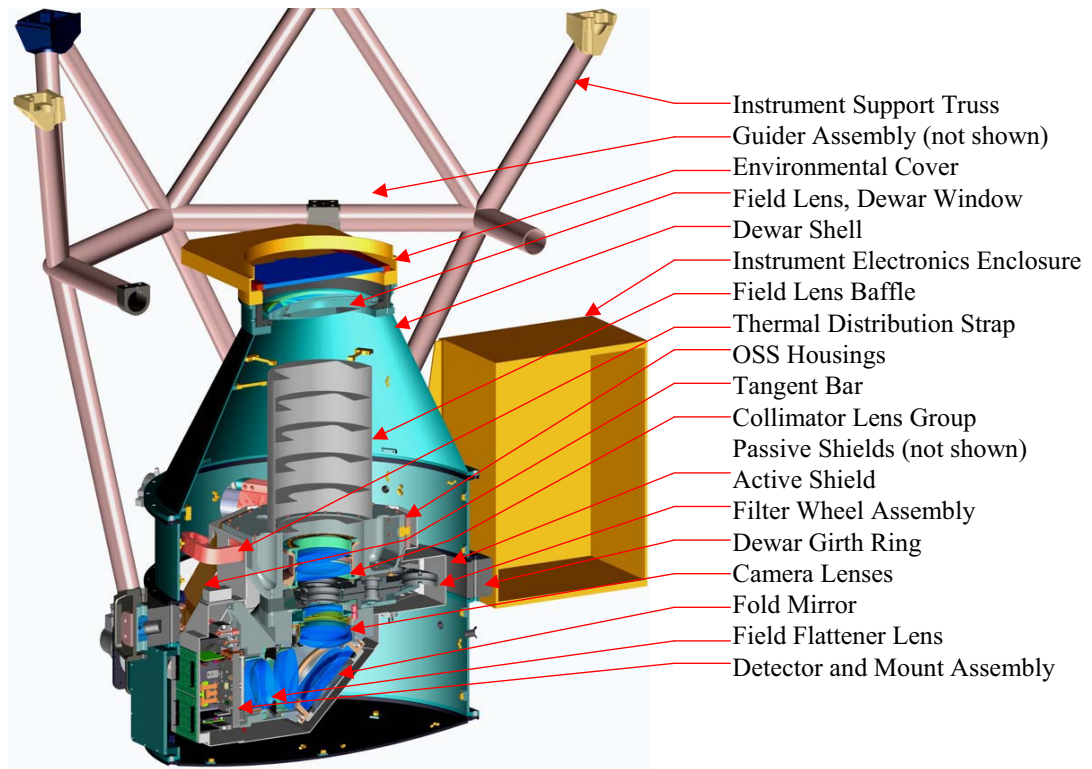


FIGURE 3.1: Cross-section view of the NEWFIRM camera. Light enters from above in this diagram, and passes through various optical elements (see labels).

The details of the observing configurations for NEWFIRM are given in Table 3.1. The camera is mounted at the Cassegrain focal station of the 4-m tele-

2. The filter properties can be viewed in the online Users Manual at <http://www.noao.edu/ets/newfirm/>.

scopes, with a converging beam as indicated in the table. The pixel scale samples the delivered point spread function (PSF) well, which is seeing-limited at all wavelengths. The image quality at the 4-m telescopes is good, with little (<10%) focus gradient or PSF variation across the field of view. The pixel scale is slightly variable from the center to the edge of the FoV due to pincushion distortions. There is very little vignetting.

TABLE 3.1: NEWFIRM Observing Configuration

	KPNO 4-m
Field of view	27' × 27'
Pixel scale of FPA	0.40 arcsec pixel ⁻¹
Inter-array gaps	35 arcsec, or 88 pixels
Delivered image quality	0.8 arcsec in excellent seeing conditions
Telescope focal ratio	f3.1

It is important to note that there is no mechanical shutter for the NEWFIRM camera; rather, the exposure duration is regulated by the difference between the initial and final nondestructive reads of the array. This has important implications for the linearity and measured counts, particularly at high count rates; see “Array Operation” on page 3-7 for details.

Focal Plane

The focal plane of the NEWFIRM Camera is populated with an array of four Orion InSb detectors, arranged in a 2 × 2 mosaic, as shown in Figure 3.2. Each of the detectors has 64 amplifiers to provide high-speed, parallel readout of the entire array as fast as 1.4 s. Representative detector properties are given in Table 3.2; most values do not differ significantly from array to array. Compared to present-day CCD detectors for the optical band, the sensitivity and dynamic range of this generation of large-format IR detectors are excellent, but the array cosmetics, noise, and linearity are inferior. The response of the NEWFIRM Orion detectors is linear to within about 6% for exposures less than 80% of the full-well. The QE varies somewhat from detector to detector, both on average and as a function of wavelength, in part due to differences in the anti-reflection coatings. (See Merrill 2008 for details.) Therefore, the transformation from instrumental magnitudes to standard systems depends upon the detector. See “Photometric Calibration” on page 3-24 and “Photometry” on page 3-29.

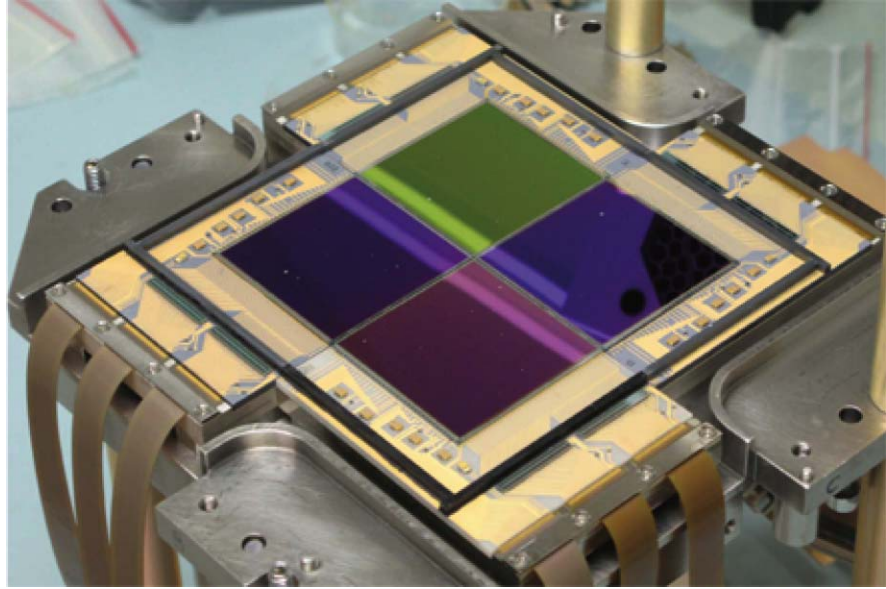


FIGURE 3.2: Mounting for the NEWFIRM focal plane array, showing the four 2048 x 2048 pixel Orion InSb detectors.

TABLE 3.2: Orion InSb Array Characteristics

Array Dimensions	2048 × 2048
Pixel Size	24 μm square
Gain	8 e^- /ADU
Read noise, RMS	35 e^- (1 Fowler sample)
Dark current	0.17 e^- / s
Well capacity	~100,000 e^-
Nonlinearity	~6% at 10,000 ADU
Read Time (Dig. Avg. = 4, Fowler samples = 1)	1.4 s

The flat-field image shown in Figure 3.3 illuminates the most significant cosmetic defects in the photo-active areas of the arrays. The spatial extent of these defects (along with the inter-chip gap) determines the minimum separation of the spatial dithers that are required during observing to mask their effect on the final, stacked images. A brief description of the defect types, numbered as in the figure, follows:

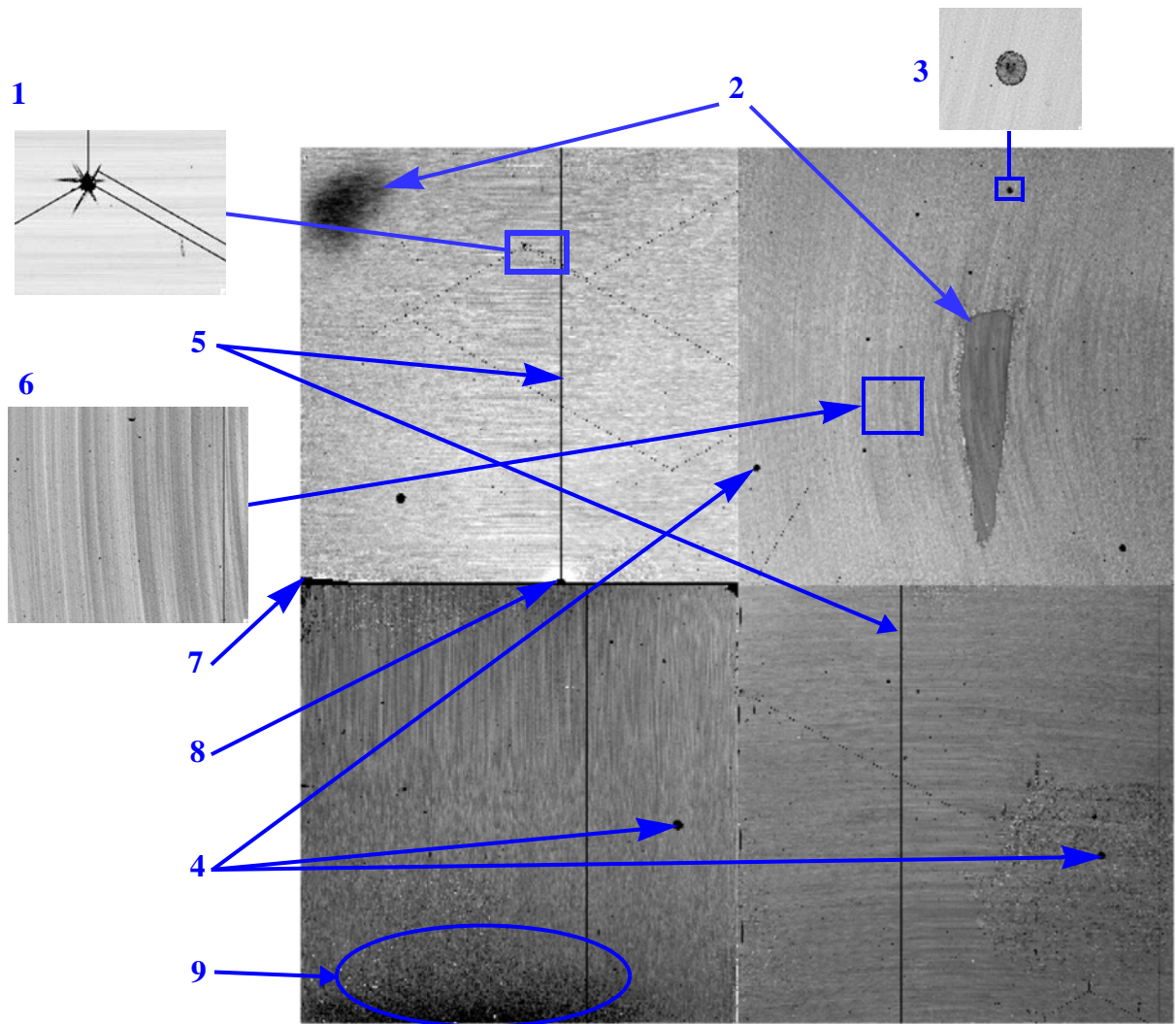


FIGURE 3.3: *H*-band Flat-field image showing all 4 arrays abutted, indicating examples of various cosmetic defects in the NEWFIRM focal plane array. See text for descriptions.

1. Diagonal cracks in the InSb substrate, where there is zero sensitivity.
2. Broad regions of slightly reduced sensitivity and higher dark current.
3. Small regions of reduced sensitivity due to contaminants on the arrays.
4. Photo-Emissive Defects (PED), which result from shorts in the bonded readout electronics, and which have been passivated at the expense of a number of roughly circular areas as large as ~50 pixels diameter with zero sensitivity.
5. Inoperable rows or columns, which are often but not always associated with a PED.
6. Residual patterns (with few-percent amplitude) of substrate crystal formation (i.e., “growth rings”), which are easily removed with the flat-field correction.

7. Regions at the detector edges or corners that have debonded from the readout electronics, resulting in zero sensitivity.
8. Damaged region on detector, with surrounding area of high dark current and nonlinear response that is masked in pipeline processing.
9. Extended regions of elevated dark count and pixel nonlinearity.

Figure 3.4 shows the arrangement of the NEWFIRM focal plane array on the sky, using the same nomenclature as is found in the FITS file extension headers.³ Note that the raw image array coordinates are remapped from the detector coordinates, such that the image origin is always in the lower-left corner when oriented as in the figure.

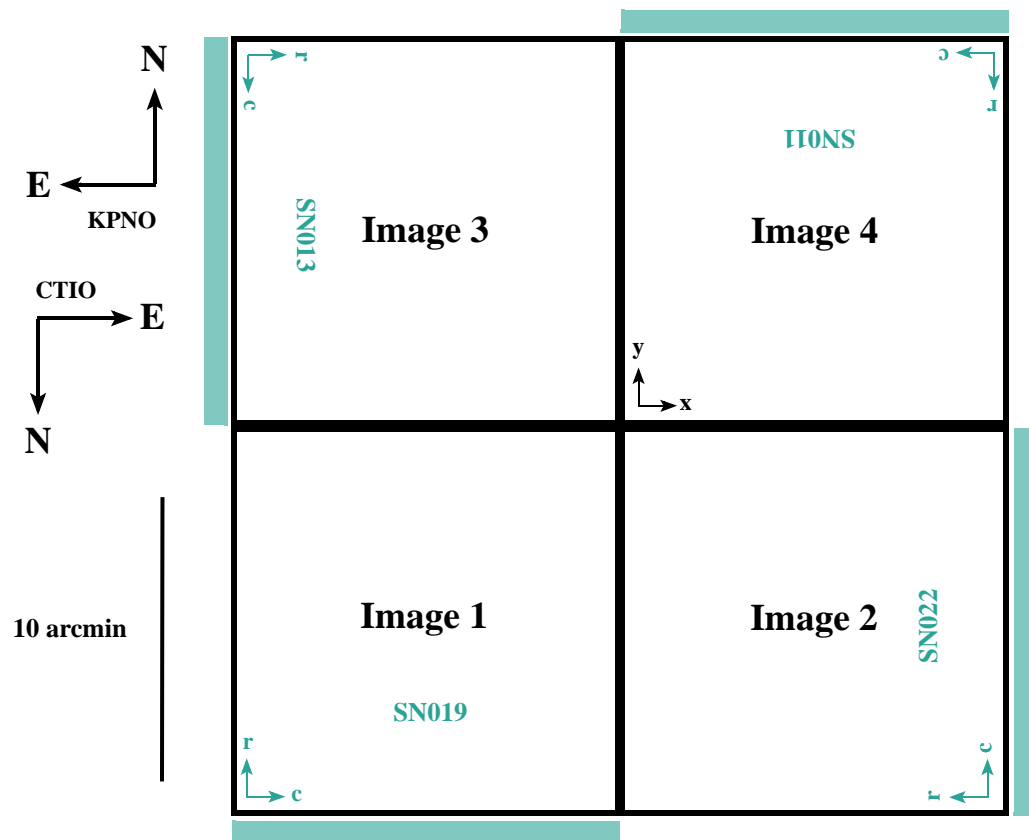


FIGURE 3.4: Orientations on the sky and spatial footprint of the focal plane array for the NEWFIRM camera, with FITS image extension and IR detector designations indicated. Coordinate (x, y) axes originate in the lower-left corner for all images (black arrows). The detector coordinate (row, column) origin is indicated for each array (teal arrows). Location of the 64 output amplifiers for each array is also indicated (teal bars). Gap between adjacent sensors is 35 arcsec.

3. The detectors and the orientation of the image arrays were changed during the course of instrument commissioning; this diagram reflects the final configuration for data obtained after semester 2007B.

3.1.2 Operations

An understanding of NEWFIRM data products requires a basic knowledge of how data are obtained during an observing run, which in turn requires knowing both how the arrays are operated and the strategies used to optimize the spatial coverage of the intended region of interest on the sky.

Array Operation

There are a few key points to bear in mind when trying to understand data from NEWFIRM. First, the exposure duration is not regulated with a mechanical shutter, as is done with CCD cameras, but is instead controlled by rapid, precisely timed, nondestructive reads of the detector array. The strategy for operating the NEWFIRM detectors is called *correlated double-sampling* (CDS), where the pixel values in the output image are in reality a *difference* between a final and an initial read of each pixel. The integration time is constant across the array, but the interval over which a given pixel integrates depends on its position on the array. This differencing also masks the fact that the pixels are accumulating counts during the finite time required to reset the array and read it out; this “hidden” flux affects the linearity correction at high backgrounds. The total elapsed time from the array reset to the last read of the last detector pixel depends upon four parameters that are set by the observer, as shown in Table 3.3. Each combination of these readout parameters changes the readout

TABLE 3.3: NEWFIRM Array Readout Parameters

Parameter	Default Value	Description
Exposure Time	—	Duration of exposure, which is the elapsed time between the first sampling of the initial readout of the array and the first sampling of the final readout of the array.
Digital Averages	4	Number of back-to-back samples of each pixel during the course of a single array read; samples are averaged to determine the raw pixel value.
Fowler Samples	1	Number of times the entire array is read just after reset, and again at the end of the integration. Resulting raw image is the difference between the sum of the last readouts and the sum of the initial readouts. Using $N > 1$ is appropriate when the S/N ratio is dominated by read noise, rather than the background.
Co-adds	1	Number of integrations taken in sequence and summed (on-board) into a single output image.

timing (see Table 3.4), the effects of which can be quite significant: at high count rates; the main effect is in the linearity correction as illustrated in Figure 3.5; at low count rates the amplitude and structure of the dark “pedestal”

is affected by the readout timing. This change in readout timing is the reason that dark frames must match the science frames with respect to the integration time and the array operation parameters in the above table; otherwise the dark frames will not accurately represent the accumulated dark current during a science exposure.



Note that raw data frames obtained with **N Fowler Samples** will, in effect, contain the **sum** of the N readouts, rather than the average. Raw data frames obtained with **M Co-Adds** will also be recorded as the **sum** of M images, although this is perhaps the expected behavior. Images calibrated by the NEWFIRM pipeline are normalized to unit exposure time.

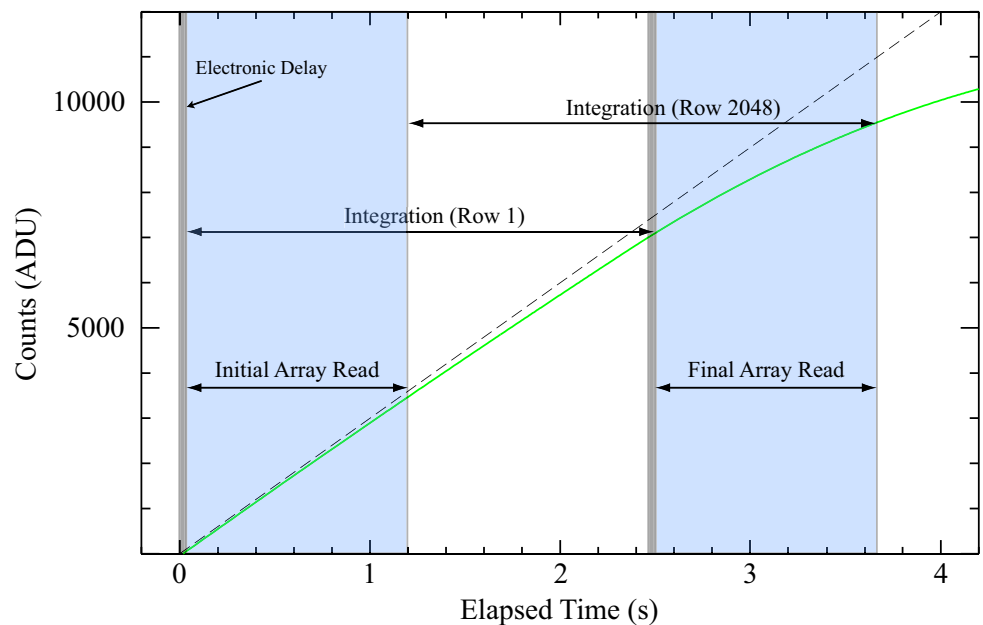


FIGURE 3.5: Schematic of the detector response (*green curve*) to a very high incident flux of 3000 ADU s^{-1} (*dashed line*) as a function of time. After the array is reset the counts begin accumulating from zero. In *correlated double-sampling*, after a brief delay the array begins reading out, which takes 1.16 s when $\text{DigAvg} = 4$ and one Fowler sample (*blue shaded regions*); following a programmed delay to achieve the integration time of 2.5 s, the detector is read again. Although the integration time is constant across the array, the interval over which a given pixel integrates depends on its position in the array.

TABLE 3.4: Array Readout Times

		Number of Fowler Samples		
		1	4	8
No. Digital Avgs.	1	0.565	1.52	2.753
	2	0.894	2.270	4.103
	4	1.195	3.014	5.439
	8	1.785	4.092	8.101
	16	2.965	7.448	13.425

Observing Sequences

Essentially, all NEWFIRM observers obtain multiple exposures of their science fields per filter; usually in a sequence of small spatial dithers about a reference position in order to obtain data in the gaps between the detectors in the FPA, and to ameliorate the effects of detector artifacts (see Figure 3.3 on page 3-5). Many observing programs also obtain sequences of (slightly) overlapping images, which enables the mapping of large regions of sky from the component images. These sequences are enabled at the telescope with a set of standard scripts, the parameters of which specify the observing pattern on the sky and the relative offsets between pointings within the pattern; these sequence parameters are written to the FITS headers of the science images.

A few of the pre-scripted observing patterns are shown in Figure 3.6, where the footprint of the NEWFIRM FPA is shown as a series of overlapping “window panes.” While the magnitude of most offsets is set by individual observers via a script, the “5PX” and “Random” patterns are most often used with small offsets to *Dither*, the “4Q” pattern positions a source of modest angular extent in the center of each detector, and the “RAxDec” pattern is used either with small offsets to dither, or with large offsets to *Map* an extended region of sky. It is also possible to obtain separate “sky” (or background reference) frames at a very large offset from an angularly very extended target (see the NEWFIRM operations manual for details). Note that these patterns can be combined: e.g., a *Dither* sequence may be executed at each position in the *Map* sequence to mosaic a large area of sky free of data gaps. The calibration pipeline will create a dithered stack of the entire map provided that the offset between map centers is no larger than 20 arcmin.

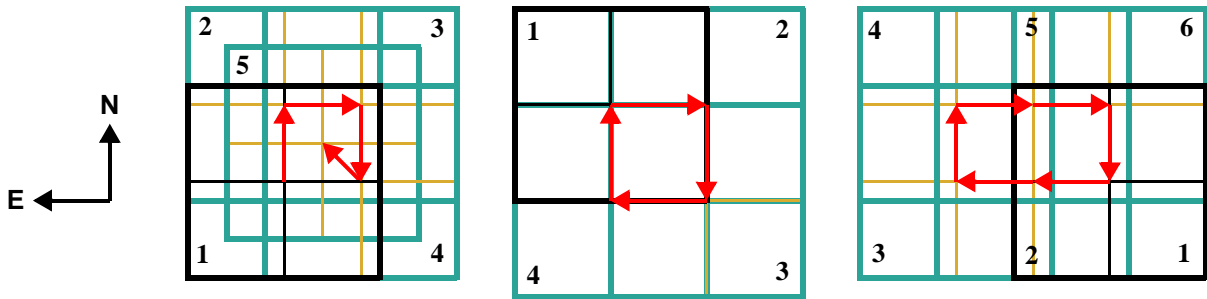


FIGURE 3.6: Schematic of three types of offset observing sequence patterns: a five-point “X” (5PX, *left*), four quadrants (4Q, *center*), and a 3 x 2 rectangle (RA x Dec, *right*) of six positions. Translation of the center of the FoV from the initial exposure in the sequence (*black footprint*) is indicated (*red arrows*).

Finally, most observing programs obtain calibration frames, such as dark frames and dome flats, using scripted sequences in order to facilitate automated pipeline processing, since the pipeline is able to recognize calibration frames from the sequence identifier. See “Calibration” on page 3-18 for a detailed discussion of how the calibration exposures are used in the data reduction process.

3.2 DATA PRODUCTS

This section describes the content and format of the various data products that are produced for the NEWFIRM camera. Most of the products are generated during the course of calibration processing, the details of which are discussed in the next section. The data products can be distinguished by the combination of the PROCTYPE, PRODTYPE, and OBSTYPE keywords in the primary header; the possible values are summarized in Table 3.5. The processing level (see Table 1.2, “Levels of Data Processing,” on page 1-4) at which the product is generated is listed in column 5 (Proc. Level).

TABLE 3.5: NEWFIRM Data Product Types and Contents

PROCTYPE	PRODTYPE	OBSTYPE	Extensions	Proc. Level	Description
Raw	image	object	IMAGE x 4	1	Raw data as obtained at the telescope, with some additional metadata included in the header
InstCal	image	object	IMAGE x 4	2	Calibrated, sky-subtracted, single-frame image
InstCal	mask	object	BINTABLE x 4	2	Bad-pixel mask for InstCal
InstCal	png	object	FOREIGN	2	Preview for InstCal
Resampled	image	object	IMAGE	2	Calibrated, sky-subtracted, re-projected image

TABLE 3.5: NEWFIRM Data Product Types and Contents (Continued)

PROCTYPE	PRODTYPE	OBSTYPE	Extensions	Proc. Level	Description
Resampled	mask	object	BINTABLE	2	Data quality mask for resampled image
Resampled	png	object	FOREIGN	2	Preview of resampled image
Stack	image	object	[None]	3	Stack of multiple, overlapping, calibrated frames with sky subtracted
Stack	mask	object	BINTABLE	3	Data quality mask for calibrated, stacked image
Stack	expmap	object	BINTABLE	3	Exposure map for calibrated, stacked image
Stack	png	object	FOREIGN*2	3	Preview for stacked image
MasterCal	image	dark	IMAGE x 4	2	Master dark calibration image
MasterCal	png	dark	FOREIGN*2	2	Preview for dark
MasterCal	image	dome flat	IMAGE x 4	2	Master dome flat-field calibration image
MasterCal	png	dome flat	FORIEGN*2	2	Preview for dome flat

3.2.1 Image Formats

The science image data from the NEWFIRM camera is stored either in FITS multi-extension files (MEFs), the general structure of which was described in Chapter 1, or in simple FITS files with no extensions. The detailed arrangement of the image portions among the extensions differs, depending upon whether the data are raw (unprocessed) or reduced.

Raw Data

Raw data from the NEWFIRM camera are organized by detector, with the output from each array stored as 32-bit integers in a separate image extension in the FITS MEF file (see Chapter 1). Thus, there are as many image extensions in the raw science file as the number of arrays in the focal plane. The coordinate origin for all images is in the lower-left corner of the readout section, rather than at the location of the first readout amplifier (see Figure 3.4 on page 3-6). This approach means that individual array images, displayed as image extensions, all have the same orientation on the sky.

The Orion detectors contain reference pixels that enable tracking the electronic stability during readout. There are actually three varieties of reference pixels on each detector, as illustrated in Figure 3.7 and Figure 3.8. The first detector column consists of pixels that electronically simulate the effect of unilluminated pixels, and the last column consists of pixels that simulate saturated pixels. There is, in addition, one reference pixel for each of the 64 parallel readout amplifiers. That reference pixel is read once for each row during the course of a

readout. The 64 amplifier reference pixels are stored at the end of each image row, as illustrated in Figure 3.7. At present, the reference pixels are not used in pipeline processing.

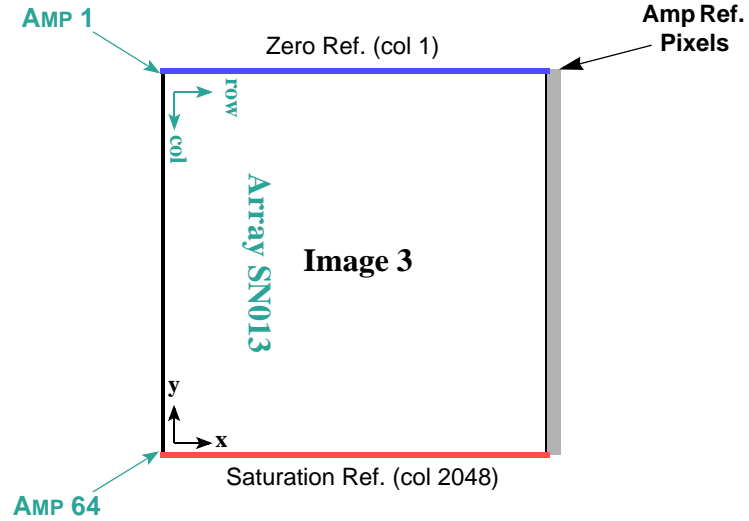


FIGURE 3.7: Schematic of the image arrays just after readout for detector SN013 of the NEWFIRM camera. Note that the image coordinates are rotated relative to the detector array. Location of the first and last of the 64 output amplifiers are indicated, as are the zero (*blue*) and saturated (*red*) detector reference columns. The photo-active region of the detector is indicated in white, while the amplifier reference pixel values, shown in grey, are stored in the highest columns of the image.

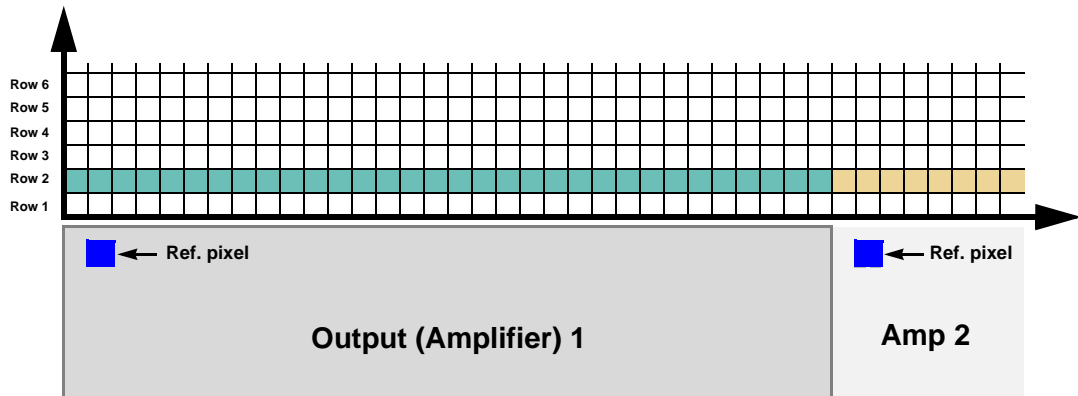


FIGURE 3.8: Schematic of a portion of the detector array illustrating the parallel readout of the second row of the IR arrays. For each row in the array, the first amplifier reads its reference pixel (fictitious locations shown in blue), followed by the first 32 pixels of the row; the second amplifier simultaneously reads its reference pixel, followed by the next 32 pixels in the row, and so on. The process is repeated for each row of the array. The values of the array reference pixels for the 64 amplifiers are stored in columns 2049:2112 of the raw image.

TABLE 3.6: Raw Data and Reference Pixel Regions

Raster Dimensions	Image	Detector	Photo-Active Data Section	Amp Reference Pixel Section
2112 × 2048	1	SN019	[1:2048, 2:2047]	[2049:2112, 1:2048]
	2	SN022	[1:2048, 2:2047]	[2049:2112, 1:2048]
	3	SN013	[2:2047, 1:2048]	[2049:2112, 1:2048]
	4	SN011	[2:2047, 1:2048]	[2049:2112, 1:2048]

Calibrated Data

The Archive contains data products that are produced with the NEWFIRM calibration pipeline. The specific calibrated science data products are given in Table 3.5 on page 3-10 and are described in more detail below. Each image has an associated *data quality mask* (DQM) and a *preview image*, which are described at the end of this subsection. The science images are stored as 16-bit scaled integers, which is a mild form of compression, when the sigma of the sky pixels can be sampled at more than 30:1 with a dynamic range over all non-flagged pixels. That is, the integer digitization has at least 30 values within 1-sigma of the sky distribution, and the 32K values span all good (i.e., non-flagged) pixel values in the calibrated data. If these conditions cannot be met, then the images are stored as 32-bit floating-point values.

InstCal. These images have been processed to remove instrumental signature and have been astrometrically and photometrically calibrated (see “Calibration” on page 3-18), although there are some cases where the calibration can fail (see “Sources of Error” on page 3-28). The pixel values have been normalized to unit exposure time (i.e., ADU s⁻¹). The data are organized in the FITS file almost identically to that for the raw science data, except for the following:

- The reference pixel regions have been trimmed from the image arrays.
- The resulting images in each extension are all 2046 × 2046 pixels containing most of the photo-active regions of the detectors.

Resampled. These images are the result of geometrically rectifying InstCal images, where each array has been re-projected to a common tangent-point on the sky, with pixels aligned to a common grid with uniform scale. The resampled image is stored in the primary header-data unit within the file. Using a common tangent-point (which is selected from a grid with roughly 1° steps in RA, and exactly 1° in Dec) facilitates stacking overlapping images within an observing sequence. The *reduced, re-projected* images are approximately 4092 × 4092 pixels; the actual size depends on the WCS tangent-point selected

for a particular image. Both the single-frame and the re-projected images are accompanied by DQMs.

Stacked. When two or more observations of a given target are obtained on the same night using the same filter and have a sufficient degree of spatial overlap (which is generally the case), these images are combined using an average with outlier rejection to remove detector blemishes, gaps between the detectors, and artifacts such as image persistence and cosmic rays. The result is a union of the spatial footprints of the stack, which is stored in a simple FITS image (i.e., not in image extensions), with nearly the same pixel scale as the raw images. These images will, in general, be larger—sometimes very much larger—than 4092×4092 pixels because the area of the sky that is mapped can be significantly larger than the instrument FoV.



The exposure duration for stacked images, as recorded in the `EXPTIME` keyword, refers to the sum of all exposure durations of all images used to create the stack. The exposure depth and noise properties of a stack, particularly from a *Map* sequence, is a discontinuous and possibly complicated function of position in the image. Use the exposure map to track the detailed exposure depth at the pixel level.

Master Calibration. Reference files are created during the course of pipeline processing: namely, darks and flat-fields. These files are used in pipeline processing to remove instrumental signatures from the science data. The Linearity Correction file is created by NOAO scientists from engineering data. See “Calibration Reference Files” on page 3-26. These reference files are 32-bit floating-point images, stored as MEF files with 4 extensions, matching the raw images.

Concomitant Data. All reduced images are accompanied by data quality masks (DQM); stacked images are in addition accompanied by exposure maps. The DQMs and exposure maps are logically images, but they are stored in compressed form as FITS binary tables, with one table per extension in the science image. Some utilities (such as the IRAF `XImtool`) can display and work with these files directly, but other utilities may require that the files be translated to FITS images before they can be used. The pixel values in the DQMs are non-zero when affected by detector pathologies and image artifacts such as bad rows or columns, saturation, and regions of passivated pixels; the values are zero otherwise. Table 3.7 on page 3-15 lists mask values that are applicable to *non-stacked* images.

TABLE 3.7: Data Quality Mask Values

Value	Meaning
0	No problem
1	Bad/invalid pixel identified in the master data quality mask; generally indicates known detector blemishes
2	Bad linearity correction
3	Saturated
4	[Not used]
5	Bad/missing background subtraction
6	Affected by detector persistence
7	[Not used]
8	Transient artifact

Most stacked images are created from dithered frames, so that most of the pathologies affecting single frames will be obviated. DQMs for *stacked* images have the following values: “1” for areas of the re-projected image with no data, “2” for areas with no data *after rejection*, and zero otherwise.

The exposure maps are images whose values are the cumulative exposure duration at each pixel, in seconds, which can be a complicated function of position for *Map* sequences (see “Observing Sequences” on page 3-9). The value of the EXPTIME keyword in a stacked image is the sum of the exposure durations for all images that contributed to the stack.

Ancillary Files. The preview images are down-sampled versions of the files they accompany and are stored in Portable Network Graphics⁴ (PNG) format. There are two samplings for each file, which are intended mainly for quick display of the results of pipeline processing on Web pages. Note that these files have been embedded in FITS files as extensions of type FOREIGN so that most users will need to extract them with some tool before viewing.

3.2.2 Header Keywords

A wide variety of metadata are recorded in the headers of the science frames. Users should browse these headers (and the extension headers) to familiarize themselves with the content. The more critical metadata are described in this subsection. Table 3.8 lists metadata by the FITS keyword name, the header unit

4. <http://www.libpng.org/pub/png/>

in which the keyword will be found (Primary or Extension), the point in the data processing where the keyword is introduced (or where the value is updated), and the meaning of the keyword (or group of keywords, if they are related). Some of the keywords are indexed by image axis, meaning they come in pairs, as indicated by the suffixes *i* and *j*.



The NEWFIRM processing pipeline is still evolving, and not all intended keywords were implemented prior to the start of data archiving in June 2009. Some keywords may be populated, but are not correctly updated by the pipeline.

TABLE 3.8: Important Science Image Keywords

Keyword Name	HDU	Origin	Meaning
Telescope			
AIRMASS	P	R	Atmospheric pathlength for target at observation start
OBSERVAT	P	R	Observatory that operates this telescope
TELESCOP	P	R	Telescope used to obtain these data
TELDEC	P	R	Declination for the telescope position on the sky in degrees
TELRA	P	R	Right ascension for the telescope position on the sky in hh:mm:ss.s
Instrument/Detector Configuration			
DETECTOR	E	R	Identifier of Orion detector in focal plane
FILTER	P	R	Filter name/designation
GAIN	E	R, U	Detector effective gain, in e^-/ADU
INSTRUME	P	R	Instrument name
NOCFSMPL	P	R	Number of Fowler samples
NOCDGAVG	P	R	Number of digital averages per pixel during readout
NOCCOADD	P	R	Number of on-board co-adds performed for this image
Image Sequences			
NOCDHS	P	R	Name of the image sequence script
NOCDITER	P	R	Dither iteration count
NOCDPAT	P	R	Name of dither pattern
NOCDPOS	P	R	Dither position
NOCDREP	P	R	Dither pattern repetition count
NOCDROF	P	R	Dither offset in RA in arcsec
NOCDDOF	P	R	Dither offset in Dec in arcsec

TABLE 3.8: Important Science Image Keywords (Continued)

Keyword Name	HDU	Origin	Meaning
NOCMITER	P	R	Map pattern iteration count
NOCMPAT	P	R	Map pattern
NOCMPOS	P	R	Map position
NOCMREP	P	R	Map repetition count
NOCMROF	P	R	Map offset in RA in arcmin
NOCMDOF	P	R	Map offset in Dec in arcmin
NOCNO	P	R	Observation number in this sequence
NOCSKY	P	R	Sky offset modulus
NOCTOT	P	R	Total number of exposures in sequence
Time			
DATE-OBS	P	R	Date and time of observation start
EXPCOADD	P	R	Duration of a single exposure in a co-add sequence, in seconds
EXPTIME	P	R	Effective exposure duration, in seconds. For stacked images the effective exposure duration can be a complicated function of position in the image.
MJD-OBS	P	R	Time of observation start in MJD
TIME-OBS	P	R	Time of observation start
TIMESYS	P	R	The principal time system for all time-related keywords. Always UTC.
World Coordinates			
CDi_j	E	R, U	Transformation matrix from pixel to intermediate world coordinates; CDi_i is the pixel scale for axis i
CRPIX i	E	R, U	Location of the reference point along axis i in units of pixels
CRVAL i	E	R, U	Value of the world coordinate at the reference point for axis i in degrees
CTYPE i	E	R	Name of the coordinate represented in axis i
DEC	P	R, U	Declination for the center of the FoV in degrees
EQUINOX	E	R	Equinox in years for the celestial coordinate system in which the positions are expressed
NAXIS i	E	R	Number of pixels along axis i
PIXSCALE i	E	R	Pixel scale along axis i in arcsec/pixel
RA	P	R, U	Right ascension for the center of the FoV in hh:mm:ss.s
RADESYS	E	R, U	Name of the reference system in which the world coordinates are expressed
WATI_ nnn	E	R, U	IRAF-specific description of the nonlinear portion of the transformation from detector to world coordinates for axis i . This character string contains coefficients for a polynomial; the length of the string is such that it must continue for nnn FITS header records.
Calibration			
BUNIT	E	L2, U	Brightness units of image (adu adu/s electron/s)

TABLE 3.8: Important Science Image Keywords (Continued)

Keyword Name	HDU	Origin	Meaning
DARKINFO	P	L2	Extent to which Dark MasterCal file matches the EXPTIME and the array sampling parameters of this science image
MAGZERO	E	L2	Magnitude corresponding to one count in the image
OBSTYPE	R	R	Type of target observed (object dark dome flat)
PIPELINE	P	L2	Pipeline name
PLVER	P	L2	Pipeline version identifier
PROCTYPE	P	L2, U	Product type (see Table 3.5 on page 3-10)
PRODTYPE	P	L2, U	Product data description (image mask expmap)
PHOTCLAM	P	L2	Central wavelength of bandpass (Å)
PHOTBW	P	L2	RMS width of bandpass (Å)
PHOTDPTH	P	L2	Photometric depth of the exposure. (See “Photometric Calibration” on page 3-24.)
PHOTFWHM	P	L2	FWHM of bandpass (Å), i.e., width measured at 50% of peak transmission
SEEING	P	L2	Average FWHM of point sources, in arcseconds
SKYBG	P	L2	Brightness level of sky background averaged over all arrays, in BUNIT
SKYBG1	E	L2	Brightness level of sky background in single array, in BUNIT
SKYNOISE	P	L2	RMS noise in the background level, in ADU

3.2.3 Environmental Data

At present no environmental data are accessible from the Archive, although data from all-sky cameras, seeing monitors, and weather conditions at KPNO are available on the Web.⁵

3.3 CALIBRATION

The current generation of pipeline processing produces Level-2 products, or images where the instrumental signature has been removed and geometric and photometric calibrations have been applied; and Level-3 products, where spatially overlapping images in the same filter (and that have been obtained within the same observing run) have been stacked. The pipeline uses calibration exposures, such as darks and dome flats taken during an observing run, to construct the calibration reference files that are used as input to the processing. For simplicity, the subsections below will first describe the processing of the science

5. http://www-kpno.kpno.noao.edu/Info/Mtn_Weather/allsky/kpasca.html

images once the calibration reference files are available; then the processes for constructing the calibration reference files will be described with the overall flow as context. The actual sequence of processing in the pipeline software differs somewhat in detail, in part to optimize the performance of the parallel processing environment.



The calibration pipeline for NEWFIRM reductions is very much tuned to maximize the use of exposures within the observing run in which they were obtained. As such, the quality of the data depends to a large degree on the quality of the calibration exposures that were obtained by the observer. However, under some circumstances the pipeline will attempt to use calibration data from prior observing runs if the separation in time is not too great.

3.3.1 Processing Steps

The flow of the science data through the pipeline is shown in Figure 3.9. Each step of the processing, indicated by the boxes in the center of the figure, is described in detail in the following subsections. Inputs to the processing include the raw science frames, calibration reference files (see “Calibration Reference Files” on page 3-26), and photometric and astrometric catalogs. Outputs include the various reduced science images, plus their associated mask files (see “Image Formats” on page 3-11). Intermediate products that are produced during the course of pipeline processing, but that are not archived, are not shown. The processing is segregated by night, filter, and further by overlapping observing sequences when deriving stacked frames.

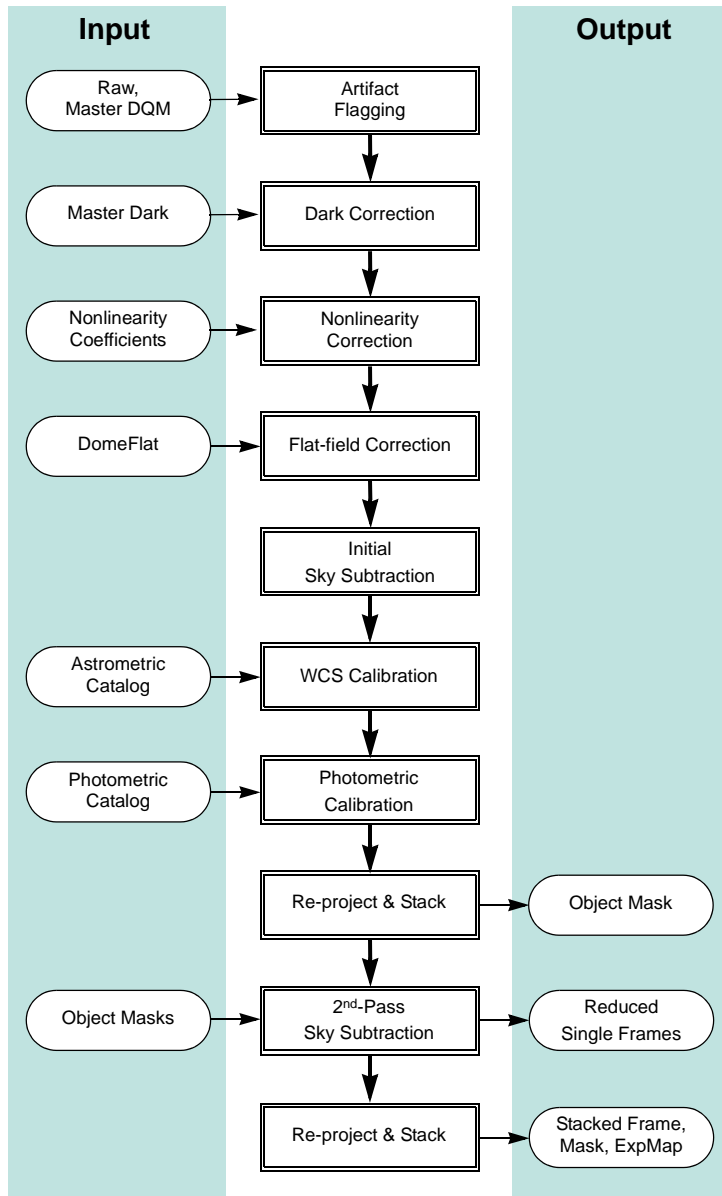


FIGURE 3.9: Flow of data through pipeline processing and calibration to produce Level-2 and Level-3 data products. External catalogs, and data products defined in Table 3.5, are shown as inputs or outputs of the processing. Intermediate products are not shown.

Artifact Flagging

Various image artifacts, including detector blemishes as described in the section on “Focal Plane” on page 3-3, are marked in the DQM of each science image. In addition, pixels with values above 8000 DN (times the product of the number of Fowler samples and Co-adds; see Table 3.3) are marked as likely to cause persistence on the next 5 images in an observing sequence. Further artifact flagging occurs later in the processing, including *saturation*, which is detected during linearity correction, and *transients* (e.g., moving objects and cosmic rays), which are detected during the final image stack. The DQM for each InstCal image indicates all detected artifacts noted above. All flagged pixels are excluded from contributing to the final, *stacked* image; if this process results in areas with no data, such pixels are so flagged (see “Concomitant Data” on page 3-14 for details).



Note that all pixels in calibrated science frames (InstCal, Resampled, and Stacked) that are flagged in the DQM with a value other than zero are replaced by a linear interpolation using adjacent pixels. The one-dimensional linear interpolation is performed along the shortest dimension of the region over which to interpolate. This process is intended to avoid introducing “ringing” artifacts during the down-stream resampling of the images, as well as to mitigate scaling problems when using image display software.

Dark Correction

The dark current, i.e., the signal introduced by thermal electrons in the detector without external illumination, is very low in the Orion arrays, and is typically $0.3 e^-/s/\text{pixel}$. However, the amplitude and structure of the dark frames is dominated by electronic bias effects, which can be a strong function of the number of on-chip co-additions, digital averages, and Fowler samples (see “Array Operation” on page 3-7), as well as the exposure time if the integrations are very short. Thus, the dark correction is applied to science frames using the Master dark frame that matches all of these parameters as closely as possible. A keyword, DARKINFO, is inserted into each science header to indicate the extent to which the master dark file matches the exposure duration and sampling type of the science exposure.

Linearity Correction

The response of the Orion infrared detectors is not perfectly linear to incident radiation, but generally can be well characterized and corrected (see Dickinson

2009). A schematic of the detector nonlinearity is shown in Figure 3.5 on page 3-8. The linearity correction for NEWFIRM is complicated by the fact that the images as recorded by the instrument do not include all the counts that accumulated in each pixel. This effect is most severe at high incident count rates and results from the method used to record the data, as described in “Array Operation” on page 3-7. In essence, counts that accumulate between the pixel reset and the first (nondestructive) read (t_r) are not reflected in the final difference image (i.e., what is recorded), but they must be accounted for when assessing where the accumulated counts fall on the linearity curve and for evaluating detector saturation. Thus, the magnitude of the linearity correction for a given pixel is dependent on a number of factors, including the number of co-adds, the incident count rate, the exposure duration, and location on the array. The linearity function is of the form $\Lambda(n) = 1 + s \cdot r_0 t$, where r_0 is the true incident count rate over total time t (which is the sum of the integration time and t_r), and s is negative. The final pixel value is the product of the measured counts and a correction factor (with a value >1.0) that takes into account the effects noted above.

Dickinson (2009) points out that the correlated double-sample (CDS) readout technique used for the NEWFIRM detectors means that detector saturation cannot be defined simply in terms of a fixed threshold of measured counts. The counts in a CDS readout will saturate at different apparent levels, depending on the intrinsic count rate, the exposure duration, t_r (see Figure 3.5 on page 3-8), and the number of co-adds and Fowler samples. It is possible to define a threshold in the context of the linearity correction, but this approach will fail at the highest incident count rates. In this regime, the affected pixels may be near saturation by the time the first readout occurs, so that the difference between the saturated second read and the initial read (i.e., the measured counts) actually declines with increasing count rate.



At very high count rates, identifying a saturation condition over broad areas of the detector (as opposed to within the cores of bright stars) is difficult to do correctly within the pipeline.

Flat-Field Correction

The flat-field correction removes the variations in the pixel-to-pixel response of the detector. In the current version of the pipeline, the flat-field is derived for each filter solely from dome-flats (i.e., images of the illuminated dome flat-field screen). The flat-field correction is performed by dividing each science frame by the flat-field calibration reference frame for the corresponding filter. The pixel values are then normalized to unit exposure time. The brightness units, as

expressed in the value of the BUNIT keyword, are ADU s^{-1} for calibrated images.

Sky Subtraction

In ground-based IR imaging, flux from the background dominates the detected signal in broadband filters from most astrophysical sources and can exceed the flux from the faintest stars and galaxies by a few orders of magnitude. The sources of the background flux include the night sky (from OH^- emission, moonlight, and a thermal component at K -band), heat sources in the telescope dome, the telescope optics, and dark current. The molecular emission in the night sky can vary significantly on few-minute timescales and can vary spatially across the large NEWFIRM FoV. Thus, highly accurate sky subtraction is essential to good photometry, and this is facilitated by relatively short exposure durations (except for narrowband filters) and spatial dithering between exposures. *It is at this stage of the pipeline that the corrections to single images generally depend upon properties derived from multiple exposures in an observing sequence.*

Determination of the sky background for individual images is a two-pass process. In the **first pass** the sky value for each pixel in the output image is determined by computing a running median with a window of up to 9 exposures in the observing sequence, excluding masked pixels in the input images and rejecting outliers to minimize the influence of transients and astrophysical sources in the stack. Note that the input images are not geometrically registered in this step: the implicit assumption is that the images are dithered, with offsets that are larger than the inter-chip gaps and detector blemishes. For sequences of 3 or fewer images, initial sky subtraction is performed by subtracting the image closest in time (i.e., pair-wise sky subtraction). For single images (not in a sequence) a smooth, low-order polynomial is fit to the background, with rejection of pixel values that are well above the background (i.e., from sources). Finally, if offset sky exposures (i.e., exposures of relatively blank sky some distance from an extended target) were *obtained as a part of the observing sequence*, these will be combined with masking and outlier rejection and used for sky subtraction of the science target. Naturally, offset sky exposures that are



Note that at present the pipeline does not provide a header keyword to indicate which type of sky subtraction was actually performed for any given reduced science image.

dithered will result in improved sky subtraction. The sky is then subtracted from each of the science images, which are then re-projected to a common geometric

frame and combined using a median with outlier rejection. The purpose of this stacked image is to create a mask for all the astrophysical sources in the field.

In the **second pass**, the source mask is unprojected to the geometry of each original (raw) image frame. The sky is redetermined using the above prescription, except that the astrophysical sources are in addition masked from the input images. The average value of the sky in units of ADUs is written to the extension headers (SKYBG1), and the average over the four arrays is written to the Primary header (SKYBG), for each calibrated science image, including the final stack.

Astrometric Calibration

The astrometric, or World Coordinate System (WCS) calibration for science images is described by a two-dimensional polynomial (the function type and coefficients are found in the header) of a tangent-plane projection of stellar coordinates to the image pixel grid. The lower-order terms relate to the location of the reference pixel on the sky, the plate scale, and the rotation of the image, while the higher-order terms relate to nonlinear effects of the optical system such as image distortion. The form and order of the function varies with the filter and to a small degree with the airmass of the observation. The initial values for all but the zero-point terms are taken from prior, full WCS solutions of calibration images where the astrometry of the stars in the field is known with very high accuracy; the initial value for the pointing is taken from the TELRA and TELDEC header keywords, which are supplied by the telescope control system.

A full WCS solution is determined for each array by associating centroids of stars in the science images with objects in the 2MASS catalog. Since the number of suitable stars in any given image (and their distribution within the image) can vary considerably, depending upon such details as the exposure time, ambient seeing, and clouds, the input list to the WCS solution includes roughly 100 additional pseudo-stars, which are merely computed points from the trial WCS solution. Thus, if the number of genuine stars in the image is small compared to the pseudo-stars, the high-order terms in the WCS solution will be dominated by the trial solution. If instead the number of genuine stars is large, they will dominate the WCS solution. In all cases, only the genuine stars contribute to determining the zero-point.

Photometric Calibration

An estimate is made of the magnitude zero-point of each science image by comparing the instrumental magnitude of each field star to their published magnitudes in overlapping passbands in a reference catalog, applying color transformations as necessary. Currently, the 2MASS reference photometric catalog is used (see Skrutskie 2006). Note that the result of the photometric calibra-

tion is to populate the science header with keywords—the pixel values remain unchanged, and have units of ADU s^{-1} .

One quantity of use, the photometric depth of the exposure, is defined as:

$$-\frac{2.5}{2.3026} \log\left(\frac{3.988 \cdot DIQ \cdot \sigma}{\sqrt{A}}\right) + m_{zero}$$

In physical terms, the photometric depth is the faintest point-source that can result in an $5\text{-}\sigma$ detection above the sky background, in units of magnitudes. In the equation above, DIQ is the delivered image quality (expressed as the value of the header keyword `SEEING` in the image header) in units of arcseconds, σ is the noise in the background in ADU , A is the area of a pixel in arcsec^2 , and m_{zero} is the magnitude zero-point. This quantity is stored in the header of the calibrated images as the value of the `PHOTDPTH` keyword.



Note the importance of the exposure time and the mean sky values that were determined during pipeline processing. These values, plus the detector gain, are stored in FITS header keywords and must be used to reconstruct the original source counts and background (in units of detected photons) when computing the statistical errors on measurements such as source magnitudes.

At present the photometric calibration is only approximate (i.e., not necessarily adequate to support science), and is most useful for the broadband JHK_s filters. For the other filters, the `MAGZERO` keyword may be useful as a rough estimate of exposure depth to support queries from the Virtual Observatory and as a measure of sky transparency over an image sequence. See “Sources of Error” on page 3-28 for details.



While the magnitudes for the 2MASS catalog are of high quality, the mapping from filters used with the NEWFIRM camera to 2MASS bandpasses, and then the color transformation from 2MASS to the nonbroadband filter set, introduces potentially significant (but uncharacterized) additional uncertainties. The resulting magnitude zero-point and photometric depth given in the headers of NEWFIRM science data are uncertain by an unknown amount that could approach 0.5 mag.

Image Re-projection and Stacking

A stacked NEWFIRM image is constructed by resampling, using a *sinc* interpolation, the component science images to a common geometric grid. Note that image blemishes and other artifacts are interpolated over in this step, so as not to cause “ringing” in the resampled images. This form of the science data product is simple to use for image stacking and transient detection, without the need to handle the distortion mapping. The astrometric system is a tangent-plane projection with a uniform sampling of $0.4 \text{ arcsec pixel}^{-1}$, oriented with North “up” (i.e., Declination increases along Axis 2) and East “to the left” (i.e., Right Ascension decreases along Axis 1). The tangent point is selected from a grid on the sky with roughly 1° steps in RA, and exactly 1° in Dec. This selection makes it easy to stack images that are part of a sequence of small spatial dithers.

When stacking, the pipeline scales the input images to a common magnitude zero-point and sky transparency. The input images are weighted by the seeing and sky brightness. The final, stacked image is a weighted average of the input images, after masking and outlier rejection.



It is common during the course of customized IR image reduction to reject images from the stack that suffer from poor image quality or unusual background levels. However, no automated mechanism for image rejection has yet been implemented in the pipeline.

3.3.2 Calibration Reference Files

The calibration reference files that are used in the pipeline processing are constructed for each observing run where a sufficient number of appropriate exposures exist. For the master flat-field reference file, the exposures that are used for calibration are affected by multiple instrumental signatures. It is important to distinguish between the additive backgrounds and the multiplicative linearity and sensitivity variations in order to avoid biasing the photometric accuracy of the processed science frames.

Master data quality masks are used to generate a DQM for each science frame that marks the locations of artifacts (e.g., inoperable rows/columns, PED dead spots, and high-valued pixels that indicate possible saturation or persistence in subsequent images). When the final, stacked calibration frames are created for each filter these artifacts are masked from the averages.

Dark

The master dark file is constructed very simply by averaging the frames after rejecting the minimum and maximum values (at least 5 dark images are required to create the reference file). Once constructed, the dark correction will be applied to all images, matching as closely as possible the exposure time, number of co-adds, and sampling type. A keyword, DARKINFO, inserted into each science header indicates the extent to which the master dark file matches the science exposure.



Since the response of the detector depends upon the rate and method of sampling the array, it is important that the master dark calibration frame correspond to the observations in exposure duration, number of co-additions, and sampling type. Significant deviations in any of these parameters will compromise the accuracy of the dark correction.

Linearity Coefficients

The linearity coefficients are derived from engineering observations that consist of a series of dome-flat exposures that were taken with a range of exposure durations such that the full dynamic range of the detectors is sampled. The intensity of the dome flat-field lamp is monitored during this sequence, and a pixel-by-pixel mapping of the measured counts as a function of illumination level may be derived. Note, however, that at the brighter illumination levels it is necessary to correct for the counts that accumulate during the “reset-to-first read” interval, as discussed in “Array Operation” on page 3-7. In the end, the pixel-to-pixel linearity curves are characterized with simple polynomial coefficients and stored in the master linearity calibration reference file. The coefficients are believed to be temporally stable and are provided to the pipeline processing system by NOAO Science staff (see Dickinson 2009).

Flat-Field

Dome flats, or exposures of an illuminated screen affixed to the interior of the telescope enclosure, are used to construct the flat-field reference file. The process for constructing the master dome flat, illustrated in Figure 3.10, begins with flagging artifacts, followed by the dark and linearity corrections on each frame. The images for each filter are then combined (with rejection of outliers and artifact rejection), separately for the illuminated and also for unilluminated frames. These “lights-on” and “lights-off” frames are then subtracted from one

another to eliminate the contribution from thermal emission even when the flat-field lights are off.⁶ The result is then normalized to an average of 1.0 over all four detectors, i.e., the ratio of the sensitivity between detectors is preserved in the flat-field, and hence is removed when applied to the science images.

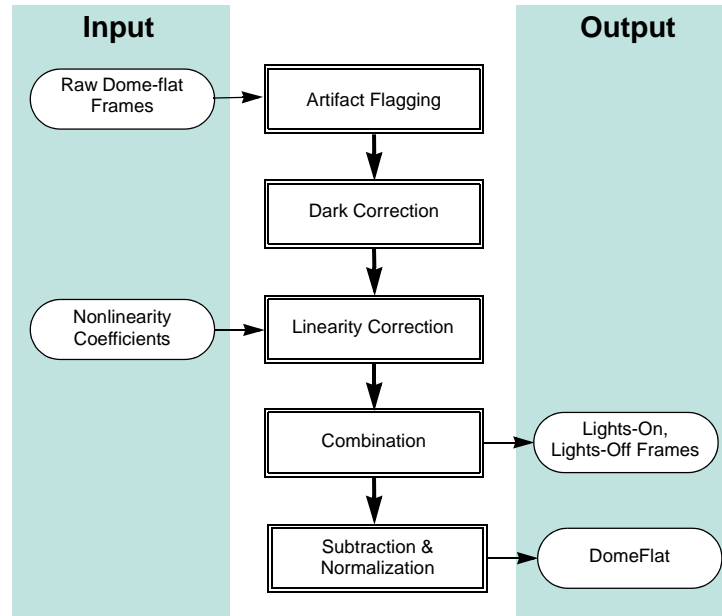


FIGURE 3.10: Process for characterizing the dome flat-field for each filter. Input dome-flat frames are uncalibrated and consist of alternating sequences with and without flat-field lamp illumination; these are combined separately and subtracted from one another.

Note that twilight- and sky-flats are neither generated nor used at present in the calibration pipeline.

3.4 SOURCES OF ERROR

This section describes the accuracy that can be expected for the major data products, the major sources of error, instrument foibles, and other noteworthy problems and issues with NEWFIRM data.

3.4.1 Astrometry

The astrometric accuracy for the image coordinate system is fundamentally limited by the science image exposure depth and the accuracy of the astrometric

6. The effect is most pronounced for *K*-band exposures.

catalog used to determine the WCS solution, which is presently that of the 2MASS catalog. This catalog has the advantage of full-sky coverage, and a limiting magnitude that provides a good overlap in the brightness range covered by most NEWFIRM exposures. Typical accuracies obtained for the WCS solution (0.2 arcsec measured in RMS deviations from the fit) are somewhat larger than the accuracy of the catalog. The geometric stability of the NEWFIRM camera has not been quantified.

3.4.2 Photometry

The photometric stability of the NEWFIRM camera has not been rigorously examined, but with care and good flat-fielding, it should be possible to achieve photometric accuracies of a few percent or better. However, **at present the photometric calibration provided by the pipeline processing is most adequate for science only with the J, H, and K_s filters**, and otherwise is intended mainly to provide an estimate of exposure depth to support queries from the Virtual Observatory. While the systematic uncertainty may be large, within a sequence of observations covering the same region of the sky, the relative uncertainties are significantly smaller and provide a useful diagnostic of the photometric stability of the sky.

The photometric performance for any given image depends mostly on a number of external factors, especially the variable sky emission and the delivered seeing. In stacked images, the photometric depth varies discontinuously across the image, so that photometric measurements of targets that span these discontinuities may suffer some additional uncertainty.

Spatial structure in the sky background is tracked implicitly by the pixel-by-pixel robust median clipping algorithm used during the two-pass sky subtraction step. However, if the actual spatial structure of the sky background is not well characterized with this technique then, photometry of extended sources may not be accurate.

3.4.3 Anomalies

Metadata

Critical metadata in raw science data files may sometimes be missing or have incorrect values. However, certain of the metadata in the headers of calibrated data, notably the WCS information and the filter name, are corrected during the course of pipeline processing (unless the calibration fails). Metadata *added* by the pipeline during processing are not in question.

Dome Lamp State

The status of the dome flat-field lamps as recorded in the header keywords is unreliable, and at present is correct only by accident. The pipeline uses a simple algorithm to distinguish between images that have been illuminated by the lamp versus those that are not. The difference is obvious except in the K_s -band.

Saturated Pixels

Pixel saturation (where the accumulated charge exceeds the full-well, e.g., in the cores of over-exposed stars) is not easy to characterize in extended regions illuminated at a high count rate. Saturated regions in flat-field exposures, for example, may not always be flagged accurately in the DQM file.

Image Ghosts

Bright stars can produce three different pupil ghosts, the effects of which may be difficult to remove. Their characteristics in the J -band filter are the following:

- A roughly 300 pixel diameter ghost, about 17 mag/arcsec² fainter than the integrated magnitude of the source star. The ghost is offset radially by hundreds of pixels with respect to the field center; the size of the offset depends upon the distance of the source from the field center.
- A roughly 100 pixel diameter ghost, about 14 mag/arcsec² fainter than the integrated magnitude of the source star, and nearly centered on it. This ghost could give rise to the appearance of false nebulosity around bright stars in stacked images.
- A compact, star-like ghost of 4 pixels diameter, which is 8.5 mag fainter than the source star and offset radially from it by hundreds of pixels, in a field-dependent manner. This ghost might appear in stacked images as bogus point sources near bright stars. But since the radial position of this ghost is field-dependent, it may be rejected from the stack if the dither pattern is sufficiently large.

Background for Narrowband Filters

Images of astrophysical targets obtained with the ultra-narrow filters (1.056 μm and 1.063 μm) contain ring-like features in the background, as shown in Figure 3.11. These ultra-narrowband filters are designed to capture the designated emission line feature with high transmission over the entire field of view at zero redshift. Owing to the convergent beam of the optical system, the filter bandpass shifts in wavelength with radial position in the FoV: at field center, the designated line falls near the blue edge of the high transmission window; at field corner, near the red edge. The “ring” features are due to the presence of OH emission lines in the night sky background near the bandpass of the narrowband filter. The bandpass shifts slightly as a function of position (distance from the

field center, in particular), and thus different amounts of the OH emission pass through the filter as a function of radius from the field center, leading to the rings.

The ring features are an additive background that varies in time. It is easily characterized, although the current version of the pipeline processing does not remove it explicitly.

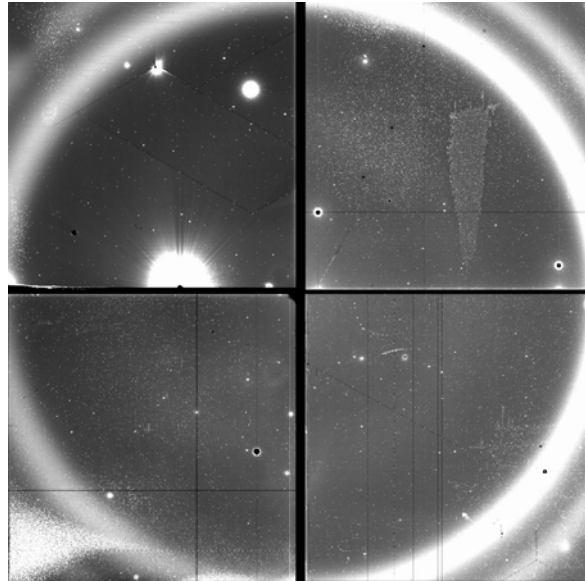


FIGURE 3.11: Image of the night sky with the 1.056 μm ultra-narrowband filter showing the “ring” feature in the background, which results from night-sky OH emission at the edge of the filter bandpass.

3.5 REFERENCES & FURTHER INFORMATION

Contributing Authors

Several people have contributed to the technical knowledge of the NEWFIRM camera. Extensive material has been contributed by Ron Probst (NEWFIRM Project Scientist) and Mike Merrill (Telescope Scientist and detector expert); by the pipeline development team of Mark Dickinson, Frank Valdes, Rob Swaters, and Tracy Huard; and by Dick Shaw. Documentation on the reduction of NEWFIRM data with the IRAF IRRED package is also fairly extensive, much of which was authored by Frank Valdes.

References

- Dickinson, M., Huard, T., Swaters, R., & Valdes, F. G. 2008, *NEWFIRM Quick Reduce Pipeline and Data Analysis Tools* (Tucson: NOAO)
- Dickinson, M. 2009, *NEWFIRM Linearity Calibration and Correction* (Tucson: NOAO)
- Fowler, A. M., & Gatley, I. 1990, *ApJ*, 353, L33
- Hoffman, A. W., Corrales, E., Love, P. J., Rosbeck, J., Merrill, M., Fowler, A., & McMurtry, C. 2008, *2K x 2K InSb for Astronomy*, *SPIE*, 5499, 59
- Merrill, K. M. 2008, *Orion SCA Laboratory Test Results Summary* (Tucson: NOAO)
- Probst, R. 2007, *NEWFIRM Quick Guide for Proposal Preparation* (Tucson: NOAO)
- Probst, R. 2008, *NEWFIRM Start-Up, Data Taking, and Error-Recovery Procedures* (Version 3.2; Tucson: NOAO)
- Probst, R. G., George, J. R., Daly, P. N., Don, K., & Ellis, M. 2008, *First Light with NEWFIRM*, *SPIE*, 7014, 93
- Skrutskie, M. F., et al. 2006, *The Two Micron All-Sky Survey (2MASS)*, *AJ*, 131, 1163

For Further Reading

A document repository⁷ for NEWFIRM is available on the Web, where many of the above-referenced papers may be found. The *JHK_s* filter bandpasses follow the Mauna Kea Observatory prescription:

Tokunaga, A. T., Simons, D. A., & Vacca, W. D. 2002, *PASP*, 114, 180

The reduction of NEWFIRM data outside the automated pipeline, including a general discussion of IRAF data reduction techniques for IR mosaics, may be found in:

Dickinson, M., & Valdes, F. G. 2009, *A Guide to NEWFIRM Data Reduction with IRAF* (Tucson: NOAO)

Additional papers on the NOAO pipeline processing system generally and the NEWFIRM pipeline in particular have appeared in the proceedings of the ADASS conference series.

7. Available at <http://www.noao.edu/ets/newfirm/>

Scott, D., Pierfederici, F., Swaters, R. A., Thomas, B., & Valdes, F. G. 2007, *The NOAO High-Performance Pipeline System: Mosaic Architecture Overview*, in ASP Conf. Ser. 376, ed. R. A. Shaw, F. Hill, & D. J. Bell (San Francisco: ASP), 265

Swaters, R. A., Valdes, F., & Dickinson, M. E., 2009, *The NOAO NEWFIRM Pipeline*, in ASP Conf. Ser., ed. D. Bohlender, P. Dowler, & D. Durand (San Francisco: ASP), in press⁸

8. Available at <http://arxiv.org/abs/0902.1458>

